cells were also able to grow in the biotinilated RAD16-I (RAD16-Ib) (**Figure 16 D**). Scanning Electron Microcopy (**Figure 16 E, F**) of the biorubber material shows a microporous structure with pore size ranging from 100 to 150 μm.

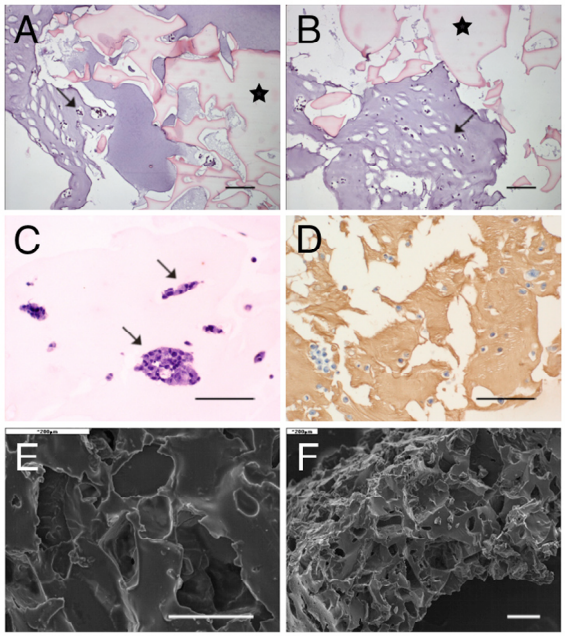

Figure 16: *In vitro* culture of cells in RAD16-I hydrogel and RAD16-I/biorubber composite.
(**A, B**) G·Luc-C57BL/6 cells suspended in RAD16-I peptide were added to biorubber and then mixed with growth medium to induce gelling of RAD16-I. Once cured, samples were fixed, dehydrated and embedded in paraffin for sectioning. Hematoxylin–eosin stained sections show cells in the RAD16-I nanofiber hydrogel (arrows) but not in the biorubber (star). (**C**) Cell clusters (arrows) in sections from RAD16-I hydrogels seeded with G·Luc-C57BL/6 cells stained with hematoxylin–eosin. (**D**) Sections from RAD16-Ib hydrogel seeded with G·Luc-C57BL/6 cells and cultivated in vitro. Biotinilated RAD 16-Ib was detected with the ABC staining, and cells by counterstaining with hematoxylin–eosin. (**E, F**) Scanning electron microscope images of freeze-fractured biorubber sputter-coated with gold. Bars: A–D = 100 μm; E, F = 200 μm.

4.2.5. Bioluminescence imaging

G·Luc-C57BL/6 cells were either, directly SC and IM implanted in BALB/c nu/nu mice, or seeded in RAD16-I hydrogel and RAD16-I/biorubber composites and then SC and IM implanted in BALB/c nu/nu mice. BLI monitoring at days 0, 7, 15, 30, 45 and 90 post implantation was used to analyze cell proliferating behavior. The captured images (**Figure 17** and **Figure 18**) show the presence of G·Luc-C57BL/6 cells at day 0 (implantation) in implants without scaffolds and with RAD16-I hydrogel scaffold, in all the animals. However, in agreement with the previous in vitro results, only 2 of 5 SC and in 4 of 5 IM RAD16-I/biorubber implants had G·Luc-C57BL/6 cells (**Figure 18 A**), suggesting that cells had difficulties penetrating and colonizing the biorubber material during the seeding period.

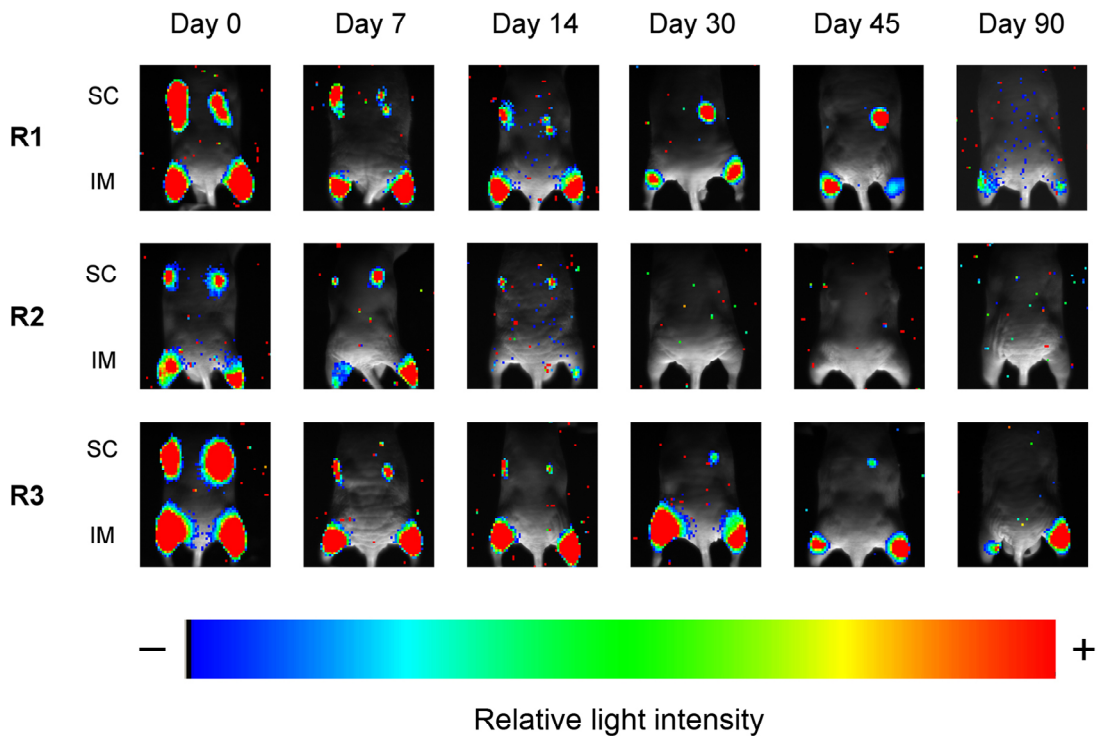

Figure 17: Proliferation of G·Luc-C57BL/6 cells *in vivo* without scaffolds.
BLI composite pseudo-colour images showing light intensity levels from SC and IM implanted G·Luc-C57BL/6 cells without scaffolds, overlaid on the corresponding white light images of mice. Colour bar shows the relative light intensity (lowest intensity = blue, highest intensity = red).

All SC implants of G·Luc-C57BL/6 cells, regardless of whether they had been implanted with or without scaffold, tended to disappear with time, as previously reported for other cell types [110], and only one of the SC RAD16-I implants retained some cells by the end of the experiment. G·Luc-C57BL/6 cells implanted IM without scaffold suffered a growth crisis 7 days post-implantation, following which the number of cells recovered to approximately that originally implanted, to then begin declining again by day 45 (**Figure 17** and **Figure 19 B, D**).

G·Luc-C57BL/6 cells seeded in RAD16-I/biorubber composites disappeared rapidly from 4 of the 5 animals with IM implants but grew well in the remaining one (**Figure 18 A**).

Conversely, G·Luc-C57BL/6 cells seeded in RAD16-I hydrogel, IM implanted, tended to grow from the beginning of the experiment in 4 of the 5 implantation sites. The difference in growth capacity between G·Luc-C57BL/6 cells seeded in the RAD16-I hydrogels and G·Luc-C57BL/6 cells implanted alone or in the RAD16-I/biorubber composites was statistically significant ($p < 0,05$) (**Figure 19 D**).

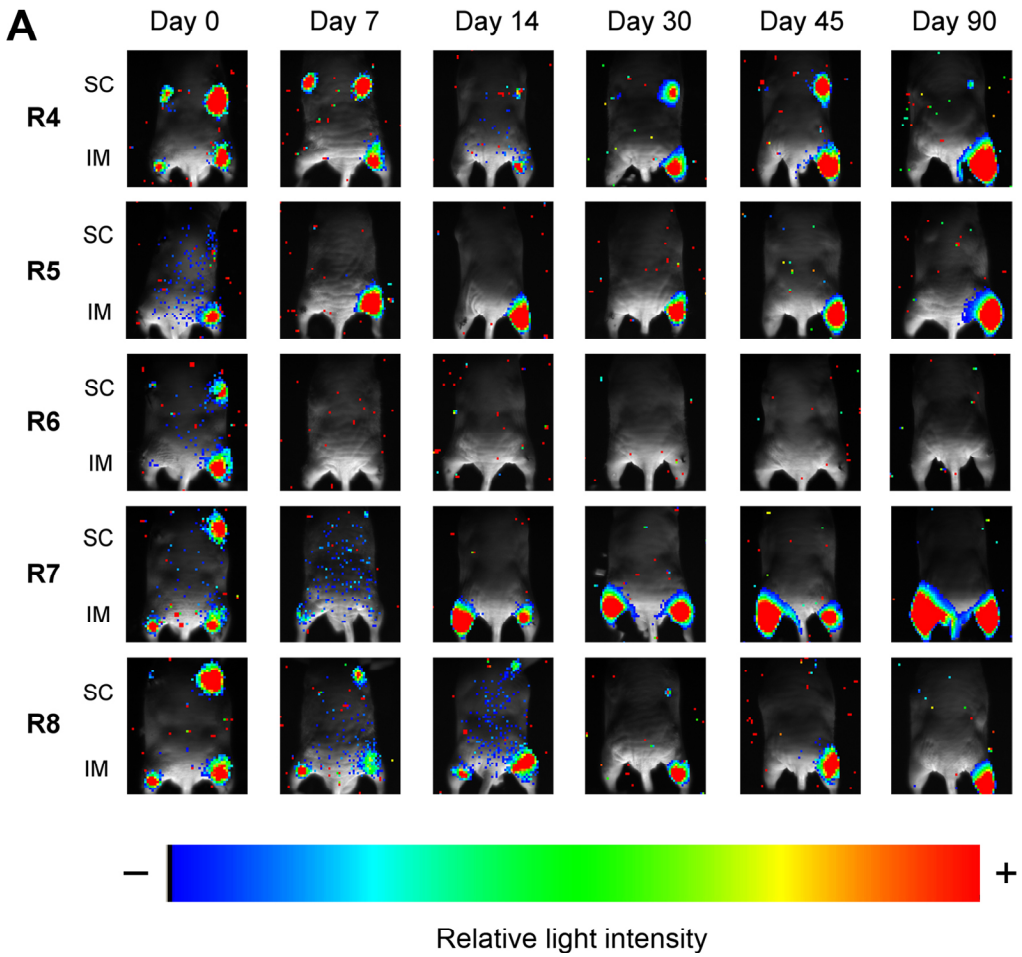

Figure 18: Proliferation of G·Luc-C57BL/6 cells seeded on RAD16-I hydrogels or RAD16-I/biorubber scaffolds.

(**A**) BLI composite pseudo-colour images showing light intensity levels of IM and SC implanted G·Luc-C57BL/6 cells seeded in RAD16-I or RAD16-I/biorubber overlaid on the corresponding white light images of mice. Colour bar shows the relative light intensity (lowest intensity = blue, highest intensity = red). (**B**) Diagram showing the location of the SC and IM implants of seeded RAD16-I and RAD16-I/biorubber composites.

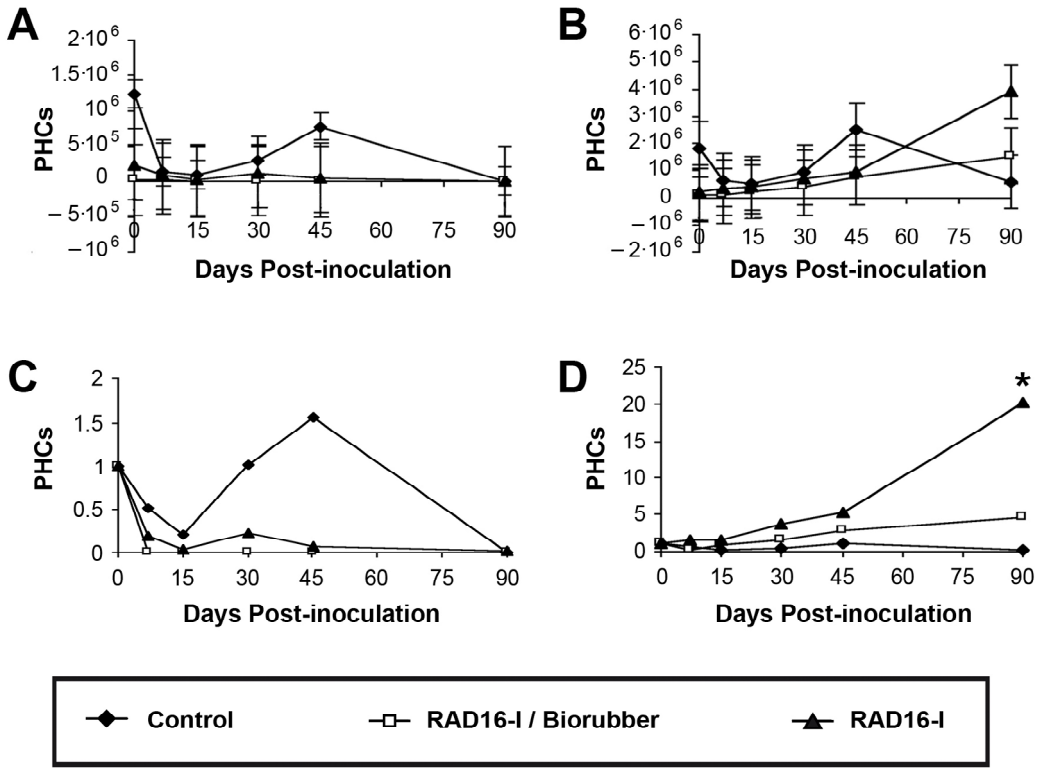

Figure 19: Quantitative analysis of BLI data.
After background subtraction of recorded photon counts (PHCs) from SC (**A**) and IM (**B**) implantations of G·Luc-C57BL/6 cells implanted without scaffold (◆) or after seeding in RAD 16-I hydrogels (▲) or RAD 16-I/biorubber composites (□), PHCs were plotted vs. time post-implantation. To compensate for differences in the seeding of scaffolds, PHCs were normalized with respect to those at day 0 (**C** and **D**). Dots represent the average value at each time point. Bars represent standard deviation, * = statistical significance ($p < 0.05$).

4.2.6. Biocompatibility of the cell constructs implanted

To determine the possible generation of immunoresponses to the biomaterials under study, RAD16-Ib hydrogel and the RAD16-Ib/biorubber composites were implanted SC and IM in six BALB/c immunocompetent mice. Implants were harvested at days 15, 30 and 45 post-implantation. No macroscopic signs of inflammation or rejection were observed in either of the implantation sites through the test. Furthermore, lymphatic nodes had normal appearance and size in all animals. Paraffin sections from the IM implants were also stained with hematoxylin–eosin (**Figure 20**), or probed with the ABC staining to localize biotin labeled RAD16-Ib. However, no signs of RAD16-Ib could be detected in the tissue sections from either early (15 days) or late (45 days) implants, indicating that the peptide scaffold had been degraded and eliminated. In contrast, the biorubber material was clearly detectable in the hematoxylin–eosin stained sections, and showed no signs of degradation while implanted in the muscular tissue (**Figure 20 A–F**) or in the SC cavity (data not shown). And although a